A novel atomic layer deposition method to fabricate economical and robust large area microchannel plates

Anil U. Mane*[a], Qing Peng[a], Matthew J. Wetstein[a,b], Wagner G. Robert [a],
Henry J. Frisch[a, b], Oswald H. W. Siegmund[c], Michael J. Minot[d], Bernhard W. Adams [a],
Matthieu C. Chollet [a] and Jeffrey W. Elam[a]
[a]Argonne National Laboratory, Argonne, Illinois 60439
[b]Enrico Fermi Institute, University of Chicago, Chicago, Illinois 60637
[c]Space Sciences Laboratory, University of California, Berkeley, California 94720
[d] Incom, Inc., Charlton, MA 01507

ABSTRACT

We demonstrate a cost-effective and robust route to fabricate large-area microchannel plate (MCP) detectors, which will open new potential in larger area MCP-based detector technologies. For the first time, using our newly developed process flow we have fabricated large area (8"x8") MCPs. We used atomic layer deposition (ALD), a powerful thin film deposition technique, to tailor the electrical resistance and secondary electron emission (SEE) properties of large area, low cost, borosilicate glass capillary arrays. The self limiting growth mechanism in ALD allows atomic level control over the thickness and composition of resistive and SEES layers that can be deposited conformally on high aspect ratio capillary glass arrays. We have developed several robust and reliable ALD processes for the resistive coatings and SEE layers to give us precise control over the resistance (10^6-$10^{10}\Omega$) and SEE coefficient (up to 5). This novel approach allows the functionalization of microporous, insulating substrates to produce MCPs with high gain and low noise. These capabilities allow a separation of the substrate material properties from the amplification properties. Here we describe a complete process flow to produce large area MCPs.

Keywords:
atomic layer deposition, capillary arrays, microchannel plate, photodetector, secondary electron emission

1. INTRODUCTION

MCPs are two dimensional arrays of microscopic channel electron multipliers. MCP-based detectors can have a combination of unique properties such as high gain, high spatial resolution, high timing resolution, and very low background rate [1-4]. MCPs can be used in a wide variety of detector applications including low-level signal detection, photo-detection, astronomy, electron microscopy, time-of-flight mass spectrometry, molecular and atomic collision studies, fluorescence imaging applications in biotechnology, field emission displays, and cluster physics[1-7]. The same MCP-based technology is used to make visible light image intensifiers for night vision goggles and binoculars[8]. In the MCP basic operation, an incident electron strikes the input wall of one pore in the MCP array causing secondary electrons to be emitted from the pore surface. With a biasing potential of ~1000V applied between the electrodes, a uniform electrostatic field is generated in each channel. This field accelerates the secondary electrons along the channel, and these electrons generate additional secondary electrons producing a cascade resulting in the emission of 10^3-10^5 electrons from the exit aperture of the pore on (Fig. 1). The MCP typically has an intrinsic resistance of 1-1000 MΩ so that current from the applied bias potential can replenish the charge on the pore walls between each amplification event.

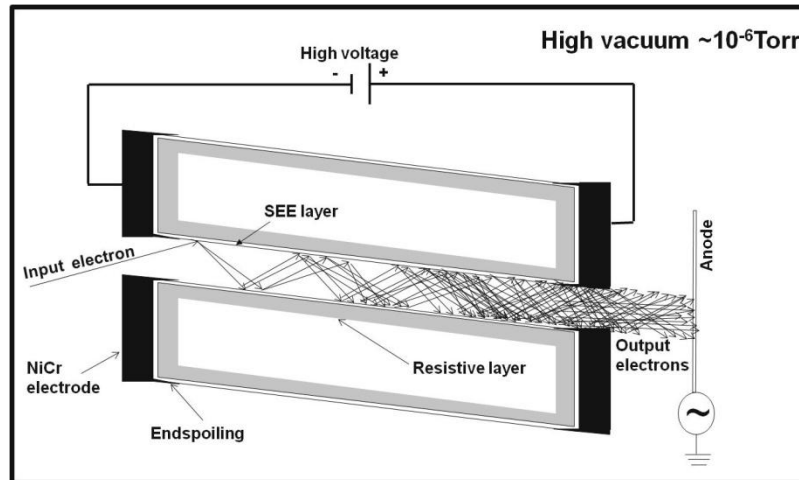*amane@anl.gov; phone 1 630 252-7014; fax 1 630 252-1342; www.anl.gov

Figure 1. Schematic of basic operation of MCP.

Recent progress in MCP readout (multi-level architecture) and high speed electronics signal processing has allowed the MCP to be used in many applications more efficiently [3, 10]. However, economical, larger area MCP manufacturing has not developed at the same pace. Increasing use of MCPs in various applications will require advances in MCP fabrication technology. Conventional MCP fabrication involves multi-fiber glass working techniques to draw, assemble, and etch an array of solid core fiber channels in a wafer of lead silicate glass. Additional thermo-chemical processing is used to activate the channel walls for electron multiplication[11]. One of the drawbacks of MCPs made using this conventional process is that the electrical conductivity and the secondary electron emission properties cannot be adjusted independently because both of these properties are imparted during the thermal activation step. Although several attempts have been made to produce MCPs with alternative processing strategies such as silicon micromachining [12, 13] and lithographic etching of anodic alumina[14], none of those technologies have matured enough to produce practical, large area MCPs. Recently, there have been efforts to improve MCP gain, resolution, and performance by functionalizing conventional, non-activated MCPs with various thin film processes[2, 14]. However, there are no detailed reports on economical, large area MCPs fabrication.

The work described here has been enabled by the convergence of two technical innovations. The first is the ability to produce large blocks of hollow, micron-sized capillary arrays being developed by Incom Inc. (Charlton, MA). The Incom process is based on use of hollow capillary, eliminating the need to remove core material by chemical etching. The arrays are fabricated as large blocks that can be sliced to form large area wafers, without regard to the conventional limits of L/d (capillary length / pore diameter). The second innovation is the advent of ALD coating methods to functionalize the capillary wafers cut from the Incom blocks. Enormous progress in thin film deposition technology, nanomaterials engineering, and rigorous process flow controls stimulated by semiconductor manufacturing offers the opportunity to improve the performance and reduce the manufacturing cost for MCP-based devices. Among these various thin film processes we have selected atomic layer deposition (ALD) for functionalizing borosilicate (non-leaded) glass capillary arrays as a route towards cost effective MCPs. ALD provides exquisite thickness control and conformality using sequential, self-limiting surface reactions between gaseous chemical precursors and a solid surface to deposit films in an atomic layer-by-layer fashion. This strategy yields monolayer-level thickness and composition control as well as continuous, pinhole-free films[15]. The self-limiting aspect of ALD leads to excellent step coverage and conformal deposition on very high aspect ratio structures. ALD processing is also extendible to very large substrates and batch processing of multiple substrates[16]. ALD utilizes gaseous molecular precursors, and they fill all the space independent of substrate geometry and do not require line of-sight access to the substrate. Material growth in ALD is also dictated by self-limiting surface chemistry. Because the surface reactions are performed sequentially, the two gas phase reactants are never mixed in the gas phase. This separation of the two reactions eliminates possible gas phase reactions that can form particles that could deposit on the surface to produce granular films[17]. All these ALD process capabilities are important for the fabrication of clean, batch-to-batch reproducible, economical, fully functionalized large area MCPs.

In this paper we demonstrate a complete process flow to produce large area MCPs. The process flow can be applied to a wide range of microchannel array substrate materials. We have chosen glass capillary arrays manufactured using non-leaded borosilicate glass because this substrate has the potential to be manufactured in large sections at low cost. To achieve high gain and fine control over the MCP performance, it is necessary to have precise control over the resistive and secondary-electron emission (SEE) layer chemistries on the MCP channels. The SEE yield is defined as the ratio of emitted secondary electrons to primary incident electrons on the examined surface. For example, the maximum SEE yield is 25 for single-crystal MgO[9].

2. EXPERIMENTAL

For MCP development work, we have used 1.2 mm thick, 33 mm diameter discs of glass micro-capillary array with pore size = 20μm, aspect ratio = 60, bias angle 8°, and open area ratio = 60% manufactured by Incom, Inc. These substrates were made from borosilicate glass multifiber micro-capillary arrays using the following steps: a) Single glass tube is heated and drawn under tension to form a hollow capillary; b) Multiple glass capillaries are assembled to form a hexagonal assembly which is heated, and drawn to form a multi-capillary bundle; c) Multi-capillary hexagonally shaped bundles are further assembled and heated under pressure to form a fused block; d) The fused block is sliced into wafers having the desired dimensions and finished (ground, polished and cleaned) to form the capillary array substrate. Prior to ALD functionalization, the substrates were further cleaned ultrasonically in acetone for 5min., followed by flushing with ultrahigh purity (99.999%) nitrogen for 30s. The cleaned substrates were placed on an aluminum channel tray with minimum contact prior to ALD costing. Silicon coupons for thickness monitors were also loaded along with the substrates in a custom made tubular ALD reactor[18]. A schematic of the MCP fabrication process flow sequence is summarized in Figure 2.
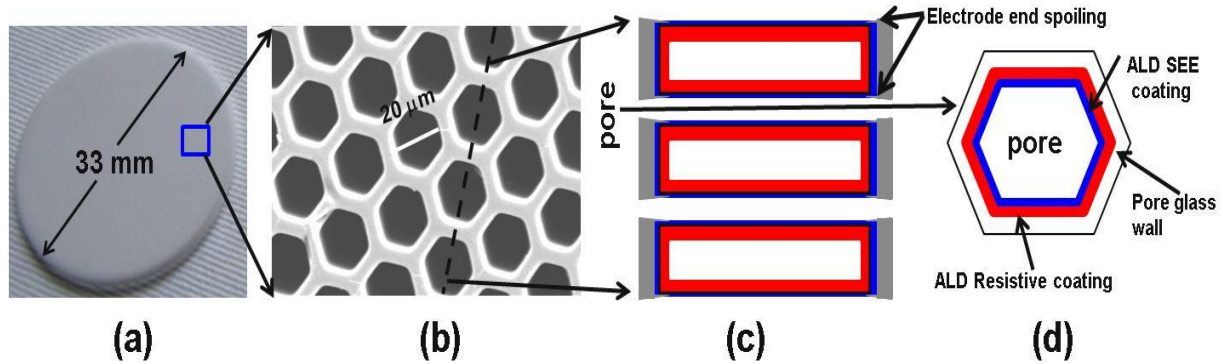

Figure 2. Fabrication sequence of MCP: (a) As received capillary glass array substrate, (b) Plan-view SEM of capillary array front surface, (c) Schematic cross section of fully-functionalized MCP, (d) Schematic cross section of individual MCP pore after ALD functionalization.

We have developed proprietary ALD processes for synthesizing resistive coatings[19]. This process is based on blending, at the atomic scale, insulating and conducting materials in the appropriate ratio to achieve a target resistivity as has been demonstrated previously[15]. The composition, and hence resistivity, of the film is dictated by the ratio of insulating and conducting components referred to as the precursor ratio. Among the several novel ALD resistive layers we have developed, the results discussed here are for the two best performing ALD resistive processes (hereafter named "chem-1" and "chem-2"). In this study we also investigated two secondary electron emission (SEE) materials, ALD Al_2O_3 and ALD MgO. All tests reported in this manuscript used combination of coatings. The highest gains were achieved using the chem-2 coating with a precursor ratio of 8% and with MgO as the SEE layer. The experimental conditions for ALD are summarized in Table 1. The thicknesses of the resistive and SEE layers were determined using spectroscopic ellipsometry measurements on the Si monitor coupons. The conformality of the resistive layer coatings on the inside the MCP channels was examined by cross-sectional scanning electron microscopy (SEM). For the electrical measurements, both sides of the MCPs were coated with 200 nm NiCr by evaporating 99.999% purity NiCr at 10^{-7} Torr vacuum conditions as described below.

To achieve the desired electrode end-spoiling, the MCP(s) were mounted such that the pore axis was aligned at 45° with respect to the NiCr evaporation source on a rotating holder. Consequently, each of the pores serve as a shadow mask such that the NiCr electrode penetrated by one hole diameter (end-spoiling=1) into each pore. The end-spoiling was confirmed by cross-sectional SEM. The MCP resistances were measured in vacuum (10^{-3}-10^{-6}Torr) using a Keithley Model 6487 Picoammeter/Voltage Source. Feasibility, process margin, and repeatability of the ALD processes were tested on several batch of MCPs. Repetitive current –voltage, long term stability and batch-to batch resistance reproducibility were also evaluated. The MCP gain and spatial uniformity of the output signal were measured in a high vacuum system equipped with a phosphor screen.

Table 1. ALD experimental parameters used for resistive and SEE coatings

	ALD Resistive layer	ALD MgO SEE layer
Deposition temperature ($^\circ$C)	200-300	200
ALD Chemistry	"Chem-2"	$Mg(Cp)_2/H_2O$
Coating thickness (nm)	93.5	7.5
Growth monitor coupons	Si(100), fused quartz	Si(100)
XRD analysis	amorphous	amorphous

3. RESULTS AND DISCUSSION

Prior to testing the chem-2 resistive layers on MCPs, a detailed investigation of the ALD process behavior such as resistivity tuning, thickness non uniformity, microstructure, and stability in air, was conducted using planar substrates. Figure 3(a) shows the thickness uniformity profile for a series of substrates coated using the optimized ALD chem-2 resistive layer grown with 8% precursor ratio on Si(100) along the flow axis of the ALD reactor. Data are shown for films grown in four separate batches. The batch-to-batch reproducibility and the thickness uniformity along the reactor are excellent. This high uniformity argues strongly for the successful scale up of this process to large area MCPs. Figure 3(b) shows cross-section SEM images collected from section of MCP, pores and wall of the pore coated under identical conditions with ~835Å of the chem-2 resistive layer. SEM confirms the deposited layer is conformal, uniform, and smooth along the pores of the MCP. Thickness measurements on the planar monitor Si(100) coupons by ellipsometry and from cross-section SEM of the pore MCP pore walls agree within the 10% uncertainty of the SEM measurements. RMS roughness estimated by atomic force microscopy (AFM) measurements from inside of the pores is <3% (image not shown).
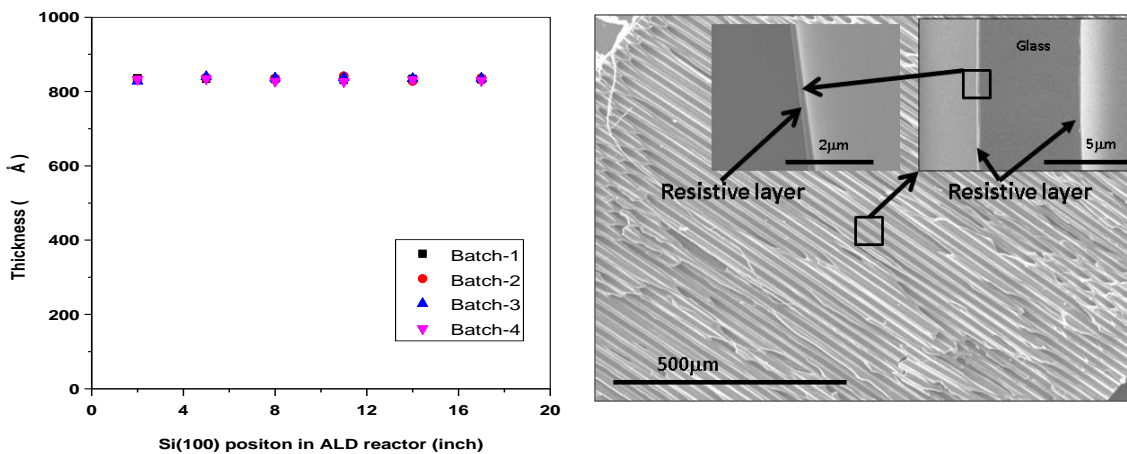

Figure 3. Thickness along the ALD reaction chamber for four identical deposition batches of chem-2 resistive layers grown with 8% precursor ratio (left image) and cross-section SEM from different regions of cleaved MCP (right image) coated with identical chem-2 resistive layer.

Fine-tuning of chem-2 layer resistivity is accomplished by adjusting the ALD precursor ratio to control the relative proportion of conducting and insulating components of the film as shown in Figure 4(a) for quartz coupons and fully functionalized MCPs. During this set of experiments all of the ALD process parameters were kept constant except for the precursor ratio. The layer resistance on quartz substrate was measured using a mercury (Hg) probe contact ring method whereas the resistance on MCPs was measured by contacting the NiCr electrodes and performing current-voltage (I-V) measurements. Under all conditions the linear I-V response was obtained for the chem-2 resistive layer. The difference between the resistivities measured on the quartz substrates and the MCPs may result from deviations between the model geometry and true geometry for the capillary array substrates, or from a slightly different composition inside of the high aspect ratio MCP compared to on the planar substrates. The resistivity of the chem-2 layer is strongly dependent on the ALD precursor ratio and this allows the resistance of the MCP to be conveniently tuned to optimize the steady-state current to suit a particular application. The resistance stability of the chem-2 resistive layer on an MCPs coated with 8% precursor ratio was tested under constant a 100V bias in vacuum at a pressure of $5x10^{-6}$ Torr for several days (Fig. 4b). We found that the MCP resistance was extremely stable during this test and exhibited only <5% resistance variation.
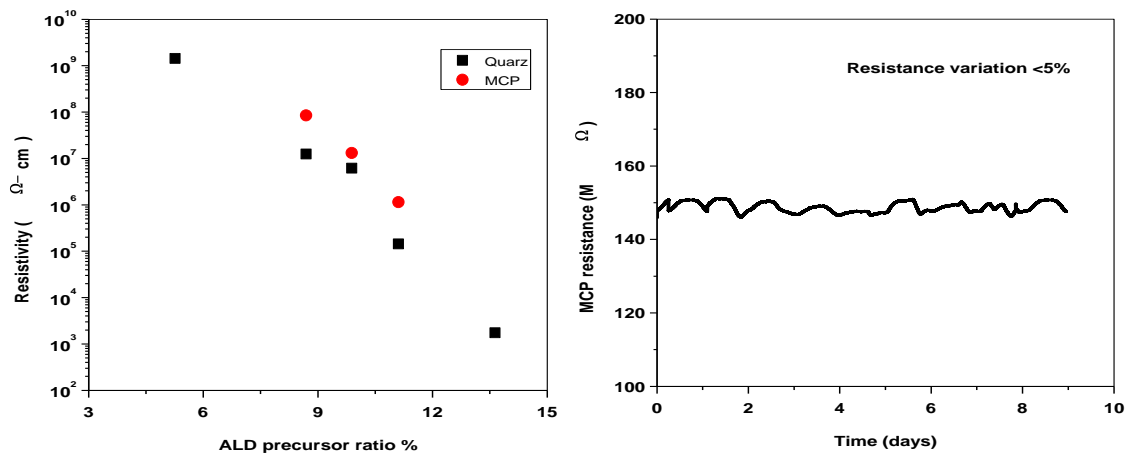

Figure 4. ALD chem-2 layer resistivity *vs.* ALD precursor ratio (a); MCP resistance stability vs. number of days under $5x10^{-6}$Torr vacuum for chem-2 resistive layer grown with 8% ALD precursor ratio (b).

The gain response with respect to applied voltage was examined for an MCP prepared using a 75Å ALD MgO SEE layer over a 935Å chem-2 resistive layer prepared using 8% ALD precursor ratio. The gain and spatial uniformity of the fully functionalized MCP were evaluated in a high vacuum system equipped with a calibrated electron source and a phosphor screen and the results are shown in Figures 5(a) and (b), respectively. The MCP gain increases monotonically with increasing bias and begins to saturate at 1200V. At 1200V bias, the gain is $3.0x10^4$. This gain value is comparable to those obtained from commercial 33mm lead glass MCPs with a similar geometry. Overall the phosphor image is fairly uniform in intensity and does not show any hot spots. The darker, hexagonal pattern visible in the phosphor image is caused by areas of lower gain, attributed to non-uniform capillary pore diameter formed during block fusion at the bond line interface between adjacent multi-capillary hexagonal bundles. Improvements in glass capillary array manufacturing are underway to minimize this effect. A comprehensive study is underway to evaluate the effects of SEE layer composition and thickness as well as resistive layer ALD precursor ratio on the overall performance of the MCPs.
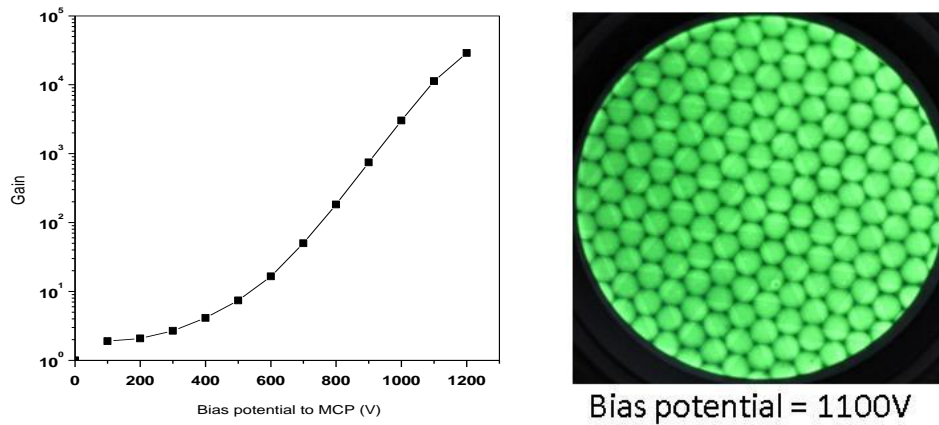
Figure 5. Gain vs. bias potential for fully functionalized MCP (a); Phosphor image with 1100V bias potential applied to MCP (b). This MCPs is coated with chem-2 resistive layer (935Å) grown with 8% ALD precursor ratio followed by 75Å MgO SEE layer

Lastly, we tested our best known MCP fabrication process on 8"x8" glass capillary array plates fabricated using the same specifications as for the 33mm plates. Photographs of the as received glass capillary substrate (a) and after ALD functionalization using the chem-1 resistive coating and Al_2O_3 SEE coating (b) are shown in Figure 6. Further work on large area MCP testing including appropriate hardware design and fabrication is in progress. We believe that the novel large area MCPs fabrication approach presented in this manuscript will offer an economical solution and new directions to detectors technology.
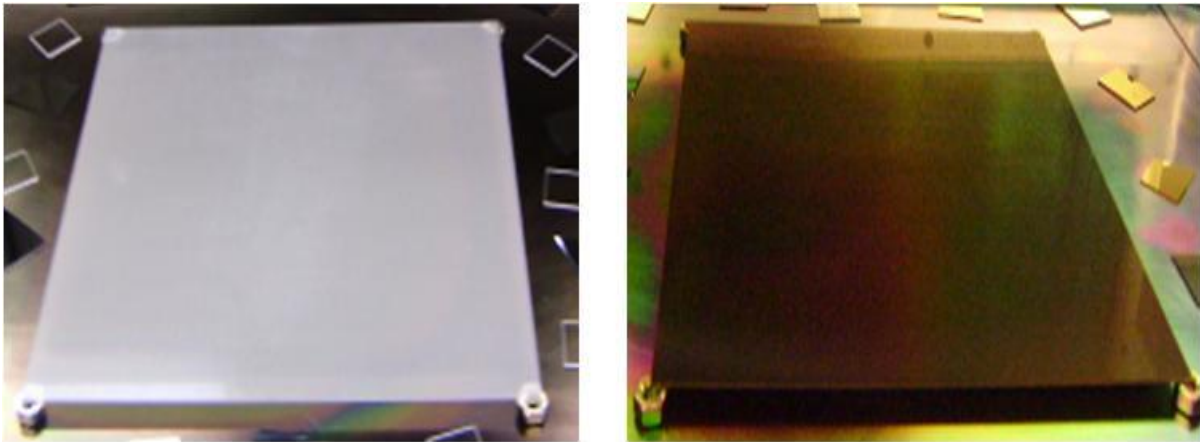

Figure 6. As received 8"x8" MCP (left) and after ALD of resistive and SEE layer (right image).

4. SUMMARY

We have demonstrated a novel process flow to fabricate large area MCPs. A newly developed ALD resistive layer shows conformal and uniform coating along the MCP pores and excellent reproducibility across multiple substrates and multiple batches. The characteristics of the resistive and SEE layers were tuned by adjusting the ALD process parameters such as temperature, composition, and precursor chemistry. Fully functionalized MCPs (33mm) fabricated by this method, show good resistance stability, repeatable performance, uniform response, and gain comparable to commercial MCPs. We have demonstrated for the first time larger area MCPs (8"x8") functionalization by our newly developed process. Further work to characterize and test the large area MCPs is in progress.

5. ACKNOWLEDGEMENTS

6. REFERENCES

[1]   Siegmund, O. H. W.; Vallerga, J. V.; Tremsin, A. S., *Hubble's Science Legacy: Future Optical/Ultraviolet Astronomy from Space*, (2003) **291**, 403.

[2]   Beaulieu, D. R.; Gorelikov, D.; de Rouffignac, R.; Saadatmand, K.; Stenton, K.; Sullivan, N.; Tremsin, A. S., *Nuclear Instruments & Methods in Physics Research Section a-Accelerators Spectrometers Detectors and Associated Equipment*, (2009) **607**, 81.

[3]   Tremsin, A. S.; Pearson, J. F.; Fraser, G. W.; Feller, W. B.; White, P., *Nuclear Instruments & Methods in Physics Research Section a-Accelerators Spectrometers Detectors and Associated Equipment*, (1996) **379**, 139.

[4]   Wenzheng, Y.; Yonglin, B.; Baiyu, L.; Xiaohong, B.; Junping, Z.; Junjun, Q., *Nuclear Instruments & Methods in Physics Research, Section A (Accelerators, Spectrometers, Detectors and Associated Equipment)*, (2009), 291.

[5]   Morichev, I. E.; Pletneva, N. I., *Soviet Journal of Optical Technology|Soviet Journal of Optical Technology|Optiko-Mekhanicheskaya Promyshlennost*, (1974) **41**, ISSN 0038.

[6]   Suzuki, Y., *Journal of the Society of Photographic Science and Technology of Japan|Journal of the Society of Photographic Science and Technology of Japan*, (1986) **49**, 294.

[7]   Yang, W.-z.; Hou, X.; Bai, Y.-l.; Bai, X.-h.; Tian, J.-s.; Liu, B.-y.; Zhao, J.-p.; Qin, J.-j.; Ouyang, X., *Acta Photonica Sinica*, (2008), 439.

[8]   Thomas, N., *Image Intensifiers and Applications Ii*, (2000) **4128**, 54.

[9]   Dekker, A. J., *Solid State Physics*, (1958) **6**, 251.

[10]   Siegmund, O.; Tremsin, A.; Vallerga, J.; McPhate, J., *Nuclear Instruments & Methods in Physics Research Section a-Accelerators Spectrometers Detectors and Associated Equipment*, (2009) **610**, 118.

[11]   Wiza, J. L., *Nuclear Instruments & Methods*, (1979) **162**, 587.

[12]   Tremsin, A. S.; Vallerga, J. V.; Siegmund, O. H. W.; Beetz, C. P.; Boerstler, R. W., *Future Euv/Uv and Visible Space Astrophysics Missions and Instrumentation*, (2003) **4854**, 215.

[13]   Xiaoming, C.; Jilei, L.; Ding, Y.; Pengliang, C.; Peisheng, X.; Shaohui, X.; Lianwei, W., *Journal of Micromechanics and Microengineering*, (2008), 037003.

[14]   Whikun, Y.; Taewon, J.; Sunghwan, J.; SeGi, Y.; Jeonghee, L.; Kim, J. M., *Review of Scientific Instruments*, (2000) **71**, 4165.

[15]   Elam, J. W.; Routkevitch, D.; George, S. M., *Journal of the Electrochemical Society*, (2003) **150**, G339.

[16]   Granneman, E.; Fischer, P.; Pierreux, D.; Terhorst, H.; Zagwijn, P., *Surface & Coatings Technology*, (2007) **201**, 8899.

[17]   George, S. M., *Chem. Rev.*, (2010) **110**, 111.

[18]   Elam, J. W.; Groner, M. D.; George, S. M., *Review of Scientific Instruments*, (2002) **73**, 2981.

[19]   Elam J. W., M. A. U., Peng Q., US patent application submitted, (2010).